PREDICTION OF TURBULENT BUOYANT FLOW USING AN RNG k-ϵ MODEL

Guohui Gan
Institute of Building Technology, Department of Architecture and Building Technology, University of Nottingham, University Park, Nottingham NG7 2RD, UK

Numerical predictions were carried out for turbulent natural convection in two tall air cavities. The standard and RNG k-ϵ turbulence models were used for the predictions. The predicted results were compared with experimental data from the literature, and good agreement between prediction and measurement was obtained. Improved prediction was achieved using the RNG k-ϵ model in comparison with the standard k-ϵ model. The principal parameters for the improvement were investigated.

INTRODUCTION

Buoyant flows occur in various engineering practices such as heating, ventilation, and air-conditioning of buildings. This phenomenon is particularly important in rooms with displacement ventilation, where supply air velocities are generally very low (< 0.2 m/s) so that the predominant indoor airflow is largely due to thermal buoyancy created by internal heat sources such as occupants and equipment. This type of ventilation system has been shown to be an effective means to remove excess heat and achieve good indoor air quality. It has been widely used in Scandinavia and Germany for ventilation of industrial and commercial buildings. The system is also gaining popularity in the UK and elsewhere for office ventilation.

Numerical studies on buoyant cavity flows were reported over a decade ago [1]. In recent years, numerical methods have been applied to computation of air movement in buildings. Most computations are based on the standard k-ϵ turbulence model developed by Launder and Spalding [2]. This turbulence model is, strictly speaking, limited to fully turbulent flows. As air movement in buildings involves both turbulent and laminar flows, a low-Reynolds-number (low-Re) k-ϵ turbulence model may provide better results of room airflow and heat transfer. Betts and Dafa'Alla [3] compared a number of low-Re k-ϵ models for predicting buoyant flow in a tall cavity but found that even the best models could not produce a completely satisfactory result. Ince and Launder [4] demonstrated that a satisfac-

Received 30 April 1997; accepted 12 September 1997.
The author is grateful to Prof. B. E. Launder of UMIST (UK) for helpful suggestions.
Address correspondence to Dr. Guohui Gan, Department of Architecture and Building Technology, Institute of Building Technology, University of Nottingham, University Park, Nottingham NG7 2RD, UK. E-mail: lazgg@unix.ccc.nottingham.ac.uk

Numerical Heat Transfer, Part A, 33:169–189, 1998

1040–7782/98 $12.00 + .00

NOMENCLATURE

C_p	specific heat of air at a constant pressure	U^+	dimensionless velocity
E	logarithmic law constant	U^*	dimensionless velocity based on wall heat flux
g	acceleration due to gravity	U_i	mean velocity component in i direction
k	turbulent kinetic energy	U_n	velocity parallel to wall boundary
L	width of cavity	U_q	velocity scale based on wall heat flux
n	normal distance of boundary grid point from wall	U_τ	friction velocity
Nu	Nusselt number	x_i	coordinate in tensor notation
p	static pressure	y^+	local Reynolds number
q	volumetric heat production/ dissipation rate	y^*	dimensionless distance normal to wall
q_w	heat flux through wall	α	thermal diffusivity of air
R	rate of strain	β	thermal expansion coefficient
Ra_H	Rayleigh number based on the height of plate or enclosure	δ_{ij}	Kronecker delta
		ϵ	turbulent dissipation rate
Ra_L	Rayleigh number based on the width of cavity	κ	Karman's constant
		λ	thermal conductivity of air
T	mean air temperature	μ	laminar viscosity of air
T^+	dimensionless temperature	μ_e	effective viscosity
T^*	dimensionless temperature based on wall heat flux	μ_t	turbulent viscosity
		ρ	density of air
T_c	surface temperature of cold wall	ρ_r	density of air at reference point
T_h	surface temperature of hot wall	σ	laminar Prandtl number of air
T_q	heat flux temperature	$\sigma_k, \sigma_t, \sigma_\epsilon$	turbulent Prandtl numbers
T_w	wall surface temperature	τ_w	wall shear stress

tory agreement with experiment data could be achieved by introducing an additional source term to the energy dissipation equation. Henkes and Hoogendoorn [5] compared numerical results by 10 different groups for turbulent natural convection in a differentially heated square cavity using the standard k-ϵ model. It was found that the wall heat transfer was overpredicted but the predicted velocity in the vertical boundary layers agreed with experiments. The prediction of wall heat transfer could be improved by inclusion of low-Re terms in the k-ϵ model. In a recent workshop on refined flow modeling [6] a comprehensive comparison of various turbulence models including low-Re models for predicting natural convection in tall cavities was presented. The results suggest that the accuracy of a numerical prediction is highly dependent on the turbulence model employed.

There are, however, limitations in applying low-Re turbulence models. For example, to achieve an accurate solution with a low-Re k-ϵ model requires a very fine grid distribution in the near-wall region and hence a significantly high computing cost. According to Laurence [7], the mesh refinement required for low-Re modeling is equivalent to what is required for direct numerical simulations. For buildings with obstructions such as occupants and furniture, if such an excessively fine mesh is also required for obstruction boundaries, it will require an extremely large number of computational cells, and so for the time being, it may not be practical to use a low-Re k-ϵ model for predicting three-dimensional flows. Also, steady solutions with low-Re k-ϵ models are limited to buoyant flows for

14. S. Garcia and E. P. Scott. Use of Genetic Algorithms in Optimal Experimental Designs, presented at 2nd International Conference on Inverse Problems in Engineering: Theory and Practice, 1996.
15. E. P. Scott, An Analytical Solution and Sensitivity Study of Sublimation-Dehydration Within a Porous Medium with Volumetric Heating, *J. Heat Transfer*, vol. 116, pp. 686–693, 1994.
16. R. E. Walpole and R. H. Meyers, *Probability and Statistics for Engineers and Scientists*, 5th ed. chap. 8, Macmillan, NY, 1993.
17. J. Guynn, Estimation of Thermal Properties in a Medium with Combined Conduction and Radiation Heat Transfer, M.S. thesis, Department of Mechanical Engineering, Virginia Polytechnic Institute and State University, Blacksburg, VA, 1996.
18. J. A. Valenzuela and L. R. Glicksman, Thermal Resistance and Aging of Rigid Urethane Foam Insulation, in *Proceedings, DOE-ORNL Workshop on Mathematical Modeling of Roofs*, Conf-811179, pp. 261–262, 1981.
19. L. R. Glicksman, M. A. Scheutz, and M. Sinofsky, Radiation Heat Transfer in Foam Insulation, *Int. J. Heat Mass Transfer*, vol. 30, no. 1, pp. 187–197, 1987.
20. M. A. Scheutz and L. R. Glicksman, A Basic Study of Heat Transfer Through Foam Insulation, *J. Cellular Plastics*, pp. 114–121, March/April 1984.
21. A. D. Belegundu, D. V. Murthy, R. R. Salagame, and E. W. Constans, Multi-Objective Optimization of Laminated Ceramic Composites Using Genetic Algorithms, in *Proceedings of the AIAA*, Paper No. 94-4364-CP, pp. 1015–1022, 1994.

Rayleigh numbers (Ra_H) up to 10^{17}, in contrast with the standard k-ϵ model, which could produce steady solutions for air up to $Ra_H = 10^{10}$ [8]. Because of such limitations, Betts and Dafa'Alla [3] considered it appropriate to use a computationally efficient means such as a wall law for calculation of recirculating flows.

Recently, Yuan et al. [9] derived wall functions for turbulent natural convection by means of dimensional analysis and experimental data. The derived wall functions were claimed to be able to produce nearly grid-independent results for airflow predictions. However, these wall functions are not universal and so have limited applications. They were derived from experimental data for fully turbulent airflow along a vertical plate. The heat transfer coefficient for natural convection, on the other hand, varies not only with the direction of fluid flow (along a horizontal or vertical or inclined surface) but also with the direction of heat transfer (to or from a nonvertical solid surface). The natural convective heat transfer to/from a horizontal surface is more important than that for a vertical surface in rooms with floor heating and, recently popular, chilled-ceiling systems. In addition, for very narrow cavities there may be interference between the boundary layers of opposing walls, where these wall functions are not applicable, as will be shown below. Furthermore, the application of such wall functions in calculations of natural convection can save only a few computational grid points in comparison with forced convection but will complicate the matching between the wall function and numerical solution [10]. As a result, the standard k-ϵ model with conventional wall functions is still most commonly used in practical engineering applications including natural convection.

In 1986, Yakhot and Orszag [11] derived a k-ϵ turbulence model using the renormalization group (RNG) theory. Since then, the model has been studied for different types of flows. For example, Nakamura and Sakya [12] used the RNG-based algebraic turbulence model to predict the transition from laminar to turbulent flow at the boundary layer. Lien and Leschziner [13] assessed various turbulent models, including the standard and RNG forms, for flow over a backward facing step. The performance of the RNG k-ϵ turbulence model for predicting buoyancy-induced turbulent flows has not been fully evaluated. Although Chen [14] showed that the RNG k-ϵ model performed slightly better than the standard k-ϵ model for indoor airflow computations, he did not show why and how the former model was superior to the latter. The purpose of the present study is to evaluate the RNG k-ϵ turbulence model in simulating buoyant cavity flows with the intention to use the model for the prediction of three-dimensional flows in occupied buildings. Comparison will be made between the standard and RNG k-ϵ models for flows in two tall cavities of different aspect ratios.

GOVERNING EQUATIONS

The governing equations for buoyant airflow are the equations representing continuity, momentum, turbulence, and temperature. In this study, the RNG k-ϵ turbulence model based on Yakhot and Orszag [11] and Yakhot et al. [15] is used. For an incompressible steady state flow the time-averaged equations in tensor notation are described as follows.

Here, σ_k, σ_ϵ, and σ_t are computed via

$$\left|\frac{\alpha - 1.3929}{\alpha_0 - 1.3929}\right|^{0.6321}\left|\frac{\alpha + 2.3929}{\alpha_0 + 2.3929}\right|^{0.3679} = \frac{\mu}{\mu_e} \tag{6}$$

Here, $\sigma_k = \sigma_\epsilon = 1/\alpha$ with $\alpha_0 = 1.0$ and $\sigma_t = 1/\alpha$ with α_0 being the laminar inverse Prandtl number ($\alpha_0 = 1/\sigma$).

R is given by

$$R = \frac{C_\mu \eta^3(1 - \eta/\eta_0)}{1 + \beta\eta^3}\frac{\epsilon^2}{k} \tag{7}$$

where

$$\eta_0 = 4.38 \qquad \beta = 0.012 \qquad \eta = \frac{Sk}{\epsilon} \qquad S = \sqrt{2S_{ij}S_{ij}} \qquad S_{ij} = \frac{1}{2}\left(\frac{\partial U_i}{\partial x_j} + \frac{\partial U_j}{\partial x_i}\right) \tag{8}$$

Temperature

$$\frac{\partial}{\partial x_i}(\rho U_i T) = \frac{\partial}{\partial x_i}\left(\frac{\mu_e}{\sigma_t}\frac{\partial T}{\partial x_i}\right) + q/C_p \tag{9}$$

where T is the mean air temperature (°C), q is the volumetric heat production/dissipation rate (W/m^3), and C_p is the specific heat of air at a constant pressure [J/(kg K)].

The density of dry air for the calculation of thermal buoyancy effect is given by

$$\rho = \frac{353.06}{(T + 273.15)} \tag{10}$$

The standard k-ϵ model differs from the RNG k-ϵ model in the following values for the empirical turbulence constants and turbulent Prandtl numbers:

$$C_\mu = 0.09 \qquad C_1 = 1.44 \qquad C_2 = 1.92$$

$$\sigma_k = 1.0 \qquad \sigma_\epsilon = 1.3 \qquad \sigma_t = 0.9 \qquad R = 0$$

In addition, for the standard k-ϵ model, the effective diffusion coefficients, μ_e/σ_k, μ_e/σ_ϵ, and μ_e/σ_t, in Eqs. (4), (5), and (9) are replaced by $\mu + \mu_t/\sigma_k$, $\mu + \mu_t/\sigma_\epsilon$, and $\mu/\sigma + \mu_t/\sigma_t$, respectively.

Boundary Conditions

The boundary conditions for solving the above equations for cavity flow include relations for momentum, heat, and turbulence at wall surfaces. For reasons mentioned above relating to the practicality of low-Re models, the following

conventional wall-function equations [2] are used for the calculation of the velocity parallel to the boundary and temperature at the boundary layer.

For $y^- \leqslant 11.63$,

$$U^- = y^- \qquad T^- = \sigma y^- \tag{11}$$

For $y^- > 11.63$,

$$U^- = \frac{1}{\kappa}\ln(Ey^-) \qquad T^+ = \sigma_t\left[U^+ + f\left(\frac{\sigma}{\sigma_t}\right)\right] \tag{12}$$

where E is the logarithmic law constant ($= 9.793$), κ is Karman's constant ($= 0.4187$), $U^- = U_n/U_\tau$ is the dimensionless velocity, U_n is velocity parallel to a boundary (m/s), $U_\tau = \sqrt{(\tau_w/\rho)}$ is the friction velocity (m/s), τ_w is wall shear stress (Pa), $y^- = \rho U_\tau n/\mu$ is the local Reynolds number, n is the normal distance of a boundary grid point from a wall (m), $T^+ = \rho U_\tau C_p(T_w - T)/q_w$ is the dimensionless heat flux temperature, q_w is heat flux through a wall (W/m^2), T_w is wall surface temperature (°C), and $f(\sigma/\sigma_t)$ is given by Jayatillaka [16]:

$$f\left(\frac{\sigma}{\sigma_t}\right) = 9.24\left[\left(\frac{\sigma}{\sigma_t}\right)^{0.75} - 1\right]\left[1 + 0.28\exp\left(-0.007\frac{\sigma}{\sigma_t}\right)\right] \tag{13}$$

For an adiabatic wall, the temperature gradient at the boundary is taken to be zero.

The near-wall turbulence energy is obtained by solving the complete transport equation for k in the near-wall control volume with modifications for the wall shear stress included in the production and dissipation terms and with the assumption of a zero normal gradient for k at the wall. The near-wall value for ϵ is prescribed with the following expression derived by assuming the production and dissipation of turbulence to be equal:

$$\epsilon = \frac{U_\tau^3}{\kappa n} \tag{14}$$

In order to assess the effect of wall functions on the accuracy of simulation, the following wall functions for turbulent natural convection proposed by Yuan et al. [9] are also used.

For heat transfer,

$$T^* = y^* \qquad y^* \leqslant 1 \tag{15a}$$

$$T^* = 1 + 1.36\ln(y^*) - 0.135\ln^2(y^*) \qquad 1 < y^* \leqslant 100 \tag{15b}$$

$$T^* = 4.4 \qquad y^* > 100 \tag{15c}$$

For momentum transfer the boundary layer is divided into inner and outer regions. The inner region is the layer between the wall and the position where the velocity

reaches the maximum value. Beyond this position and up to the edge of the boundary layer is the outer region. The wall function for velocity distribution is

$$U_i^* = 1.41 y_i^* - 3.11(y_i^*)^2 + 2.38(y_i^*)^3 \qquad y_i^* \leq 0.53 \qquad (16a)$$

$$U_o^* = -0.458 - 0.258 \ln(y_o^*) - 0.02425 \ln^2(y_o^*) \qquad 0.005 \leq y_o^* \leq 0.1 \qquad (16b)$$

$$U_o^* = 0.0 \qquad y_o^* > 0.1 \qquad (16c)$$

where $T^* = (T_w - T)/T_q$ is dimensionless temperature, $T_q = \{[q_w/(\rho C_p)]^3/(g\beta\alpha)\}^{1/4}$ is heat flux temperature, β is the thermal expansion coefficient (1/K), α is the thermal diffusivity of air (m^2/s), $U^* = UU_q^3/U_\tau^4$ is dimensionless velocity with subscripts i and o for the inner and outer regions, respectively, $U_q = [g\beta\alpha q_w/(\rho C_p)]^{1/4}$ is the velocity scale based on heat flux, $y^* = U_q n/\alpha$ is dimensionless distance normal to the wall, $y_i^* = y^* U_q^2/U_\tau^2$, is dimensionless distance for the inner region, and $y_o^* = y^* U_q^6/U_\tau^6$ is dimensionless distance for the outer region.

Solution

The governing equations are solved for the three-dimensional Cartesian system using the SIMPLE algorithm [17]. The overall structure of the computer program follows a two-dimensional TEAM computer code [18]. The original two-dimensional code is modified for simulations of buoyant airflow in enclosures.

VALIDATION

Validation of the computer code was first performed by comparing numerical predictions with the experimental results for turbulent natural convection in a narrow tall cavity by Betts and Bokhari [19]. Figure 1 shows the elevation of the cavity. The internal dimensions of the cavity were 2.18 m high, 0.0762 m wide, and 0.52 m deep. Temperatures of cold and hot walls were controlled at 15° and 35°C, respectively, for $Ra_L = 0.86 \times 10^6$ and at 15° and 55°C, respectively, for $Ra_L = 1.43 \times 10^6$. Top, bottom, front, and back walls were insulated. The Rayleigh number, Ra_L, is defined as

$$Ra_L = \rho g \beta (T_h - T_c) L^3/\mu\alpha \qquad (17)$$

where T_h and T_c are the temperatures of hot and cold walls (°C), respectively, and L is the width of the cavity (m).

Air velocities in the cavity were measured using a He-Ne single-channel laser-Doppler anemometry system. Thermocouples (type K) were used for temperature measurements. Details of the measurement are given in Ref. [20].

The experimental results indicated that flow in the central region was close to two-dimensional. Therefore conditions on the elevation (Figure 1) were used as a two-dimensional flow. The grid distribution near the wall surface is generally important for numerical accuracy. When the air temperature gradient is evaluated at the wall for calculating wall heat transfer, at least the first inner grid point

should lie in the viscous region. However, if the grid points other than the first are too close to the wall, the equations for turbulent flow, unless incorporating a low-Re model, may inappropriately be applied to the viscous region. On the other hand, if the first inner grid point is placed outside the buoyancy-induced boundary layer, using wall functions will result in unreliable flow predictions. The optimum position of the inner grid point for predicting buoyant flow using k-ϵ models is thus near the outer edge of the viscous region ($y^+ = 3$–5) so that the next computational grid point is just beyond the region. A nonuniform Cartesian grid of 39×35 was therefore generated for the simulations. The effect of grid dependence was tested by doubling the number of grid points, which produced the same velocity and temperature distributions as the original grid.

A comparison between the predicted and measured results at cavity mid-height for the two cases is given in Table 1. Air temperature at 0.1 cavity width rather than a value at the cavity center is used for comparison because the temperature difference between predictions is most obvious in the region between the wall surface and the distance of 0.2 cavity width, whereas the predicted value at the cavity center is equal to the average of hot and cold wall temperatures. Nusselt numbers along the cold and hot walls (Nu_c and Nu_h, respectively) are used to assess wall heat transfer. The Nusselt number is determined from

$$Nu = \frac{q_w}{T_h - T_c}\frac{L}{\lambda} = \frac{(\partial T/\partial x)_w L}{T_h - T_c} \tag{18}$$

where λ is the thermal conductivity of air [W/(m K)].

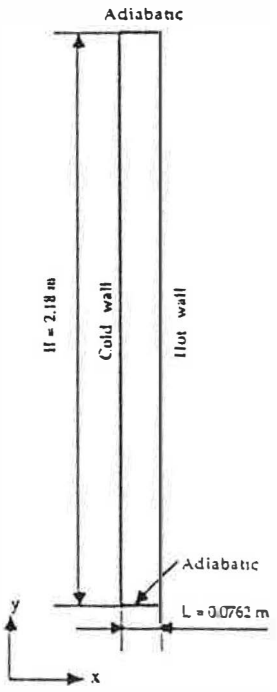

Figure 1. Dimensions of the elevation of a narrow cavity.

Table 1. Vertical velocity (V_{min}, V_{max}), Nusselt number (Nu_c, Nu_h), and temperature at 0.1 cavity width (T_1) at midheight of narrow cavity

Method	$Ra_L \times 10^{-6}$	V_{min}, m/s	V_{max} m/s	Nu_c	Nu_h	T_1, °C
Measurement	0.86	−0.135	0.139	6.24	5.91	21.7
RNG k-ϵ	0.86	−0.135	0.136	6.99	6.83	21.7
RNG k-ϵ[a]	0.86	−0.122	0.123	6.77	6.56	21.7
Standard k-ϵ	0.86	−0.118	0.119	7.12	6.95	21.6
Standard k-ϵ[a]	0.86	−0.105	0.106	6.93	6.73	21.6
Measurement	1.43	−0.189	0.190	7.85	7.45	29.4
RNG k-ϵ	1.43	−0.184	0.186	8.49	8.08	29.2
RNG k-ϵ[a]	1.43	−0.163	0.166	8.04	7.71	29.1
Standard k-ϵ	1.43	−0.161	0.163	8.68	8.21	29.0
Standard k-ϵ[a]	1.43	−0.141	0.144	8.18	7.82	29.0

[a] Based on the wall functions for natural convection.

Figures 2 and 3 show the comparison between the predicted and measured velocity and temperature profiles at the midheight of the cavity using the two k-ϵ models with the conventional wall functions at two Rayleigh numbers. In Figures 2*b* and 3*b* the dimensionless temperature is defined as $(T - T_c)/(T_h - T_c)$.

The predicted velocities (both peak values and profiles) using the RNG k-ϵ model are very close to the measured values and are much better than the predictions using the standard k-ϵ model. The standard k-ϵ model underpredicts the magnitude of maximum and minimum vertical velocities. Consequently, the predicted velocity gradients outside the boundary layers are smaller than the measurements. It is observed that the magnitude of maximum vertical velocity differs slightly from that of minimum vertical velocity. The difference is due to the variable thermal properties of air (as a function of temperature) such as thermal conductivity and laminar viscosity. This is also true for the difference in wall heat transfer (Nusselt number) along the cold and hot walls as discussed below.

Despite the marked difference in predicted velocities, the temperature profiles predicted by the two models are in excellent agreement with the measurements. Quantitatively, however, there is a slight difference between temperature results from the two models. For example, at $Ra_L = 0.86 \times 10^6$, the RNG k-ϵ model predicts the temperature at 0.1 cavity width (at cavity midheight) of 21.7°C, same as the measured value, whereas the standard k-ϵ model produces a slightly lower value of 21.6°C. The prediction of temperature using the RNG k-ϵ model is therefore marginally better than that using the standard k-ϵ model. Betts and Dafa'Alla [3] also showed a similar phenomenon, i.e., significant difference in predicted velocity (over 100%) but much less so in temperature profile using different low-Re k-ϵ models. In addition, they observed that models predicting low values of velocity predicted high Nusselt numbers.

Table 1 indicates that the wall heat transfer is overpredicted by the two models. However, similar to the predictions of velocity and temperature, the Nu predicted by the RNG k-ϵ model is closer to the measured result than is the predicted value from the standard k-ϵ model. The predicted Nu here is based on

the temperature difference between the wall surface and the first inner grid point, which is in the viscous region. The measured Nu in Table 1 is, however, obtained from the temperature gradient at the wall for data up to about 2 mm from the wall surface where the temperature profile is linear. If the same number of data points were used for the determination of Nu, i.e., the wall surface temperature and the air temperature at a position nearest the wall, the measured Nu at Ra_L of 0.86×10^6, for instance, would be greater than 8.0 for both walls, as a consequence of experimental uncertainty of the temperature measurement.

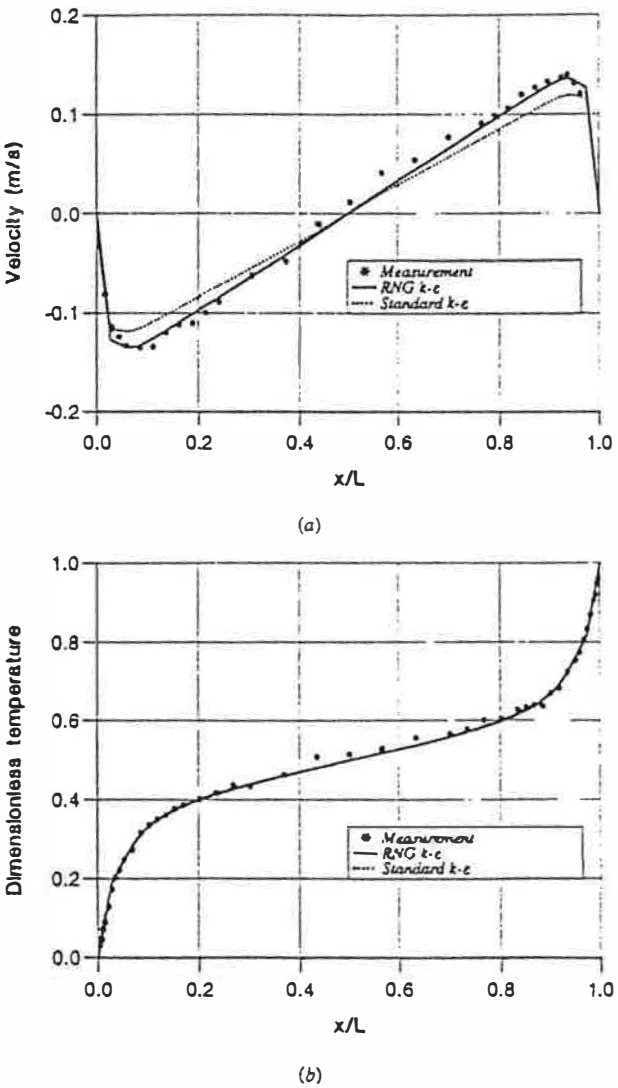

Figure 2. Predicted (*a*) velocity and (*b*) temperature at midheight in the narrow cavity using conventional wall functions ($Ra_L = 0.86 \times 10^6$).

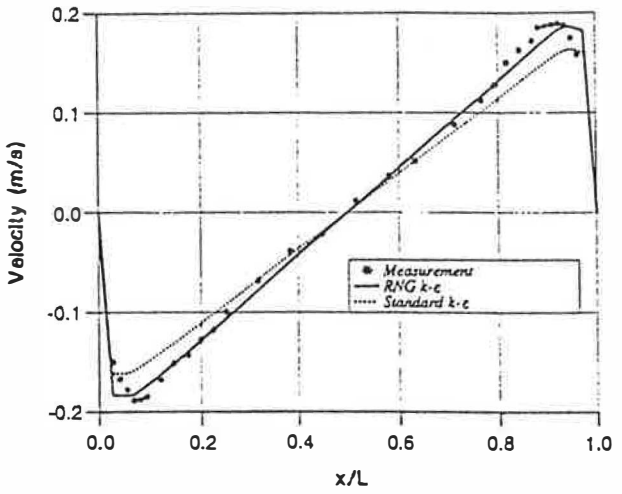

(*a*)

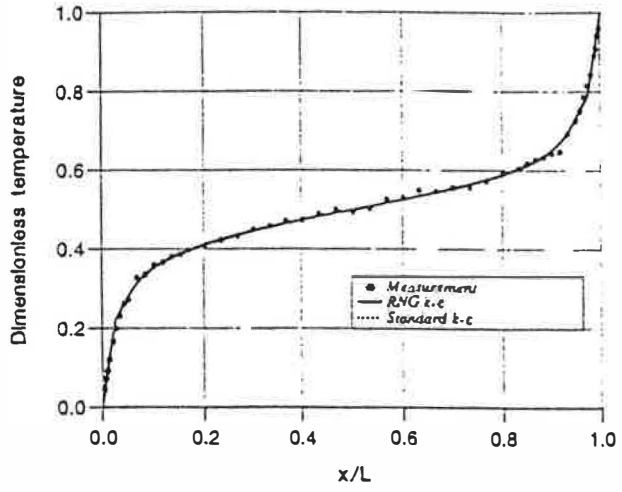

(*b*)

Figure 3. Predicted (*a*) velocity and (*b*) temperature at midheight in the narrow cavity using conventional wall functions (Ra_L = 1.43×10^6).

By comparing Figure 4 with Figure 2 and Figure 5 with Figure 3, it is seen that the predicted velocities using the wall functions for turbulent natural convection are lower than those using the conventional wall functions for shear flow. Again, the predicted temperature profiles using the two types of wall functions are almost the same. The difference in wall heat transfer between them is also small (see Table 1). Since the wall functions for turbulent natural convection could not predict the velocity magnitude in such narrow cavities as well as the conventional wall functions, their applications may be very limited. One of the possible reasons

for the poor performance of such wall functions is interacting boundary layers. Because the opposing wall is such a short distance away, it could interfere with the boundary layer of a vertical wall. Thus the near-wall boundary layer is not exactly a free convection layer as assumed for a vertical plate.

To examine this possibility, numerical predictions were also carried out for turbulent natural convection in a large rectangular cavity of 5:1 aspect ratio by Cheesewright et al. [21]. The computations were made for the case with a temperature difference between the hot left and cold right walls of 45.8 K. Figure 6

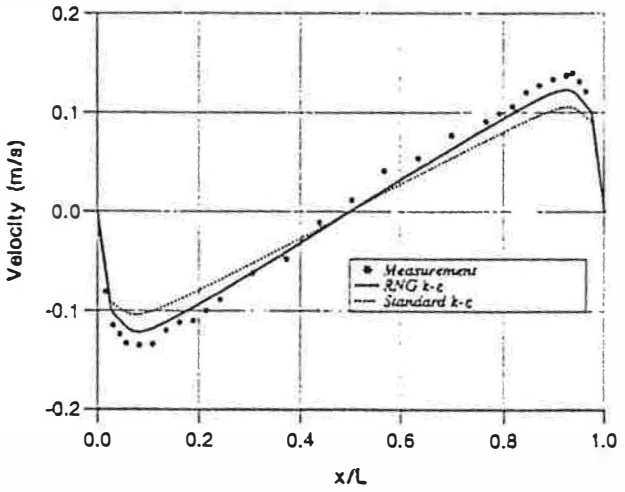

(a)

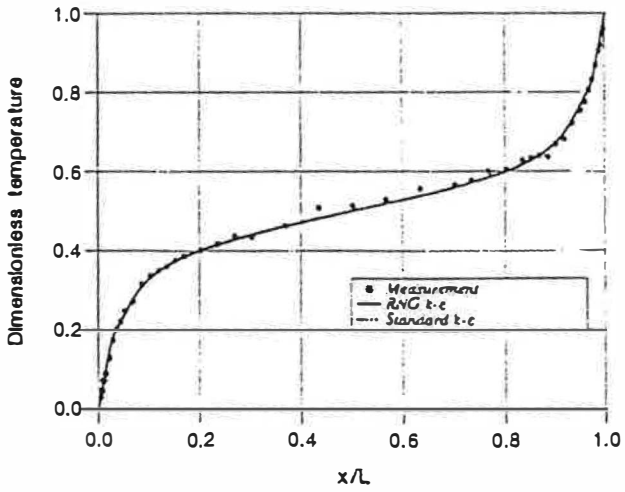

(b)

Figure 4. Predicted (*a*) velocity and (*b*) temperature at midheight in the narrow cavity using wall functions for natural convection ($Ra_L = 0.86 \times 10^6$).

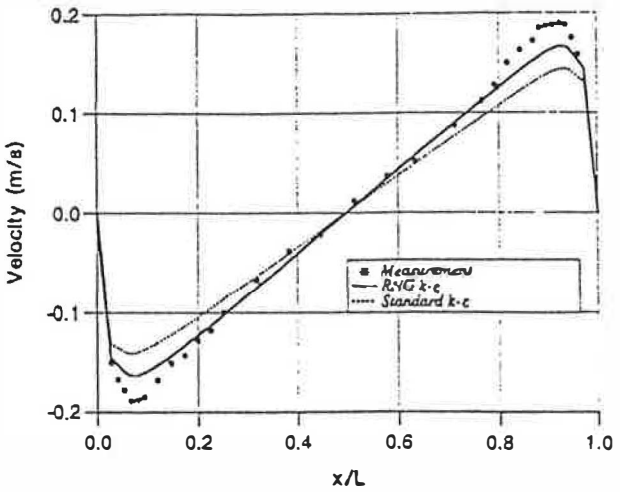

(a)

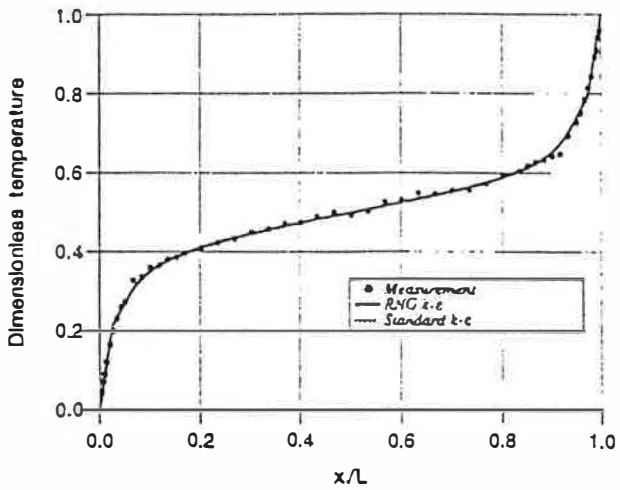

(b)

Figure 5. Predicted (a) velocity and (b) temperature at midheight in the narrow cavity using wall functions for natural convection ($Ra_L = 1.43 \times 10^6$).

shows the comparison between the predicted and measured velocity profiles at the midheight and vertical temperature distribution in the core of the cavity. It is seen that the predicted peak velocities using the wall functions for turbulent natural convection are again lower, though to a lesser extent, than those using the conventional wall functions but in this case agree slightly better with the experimental measurement. With regard to the effect of turbulence models, Figure 6a indicates that the predicted velocity profiles, other than the peak values using the RNG k-ϵ model, are in closer agreement with the measurement than the predic-

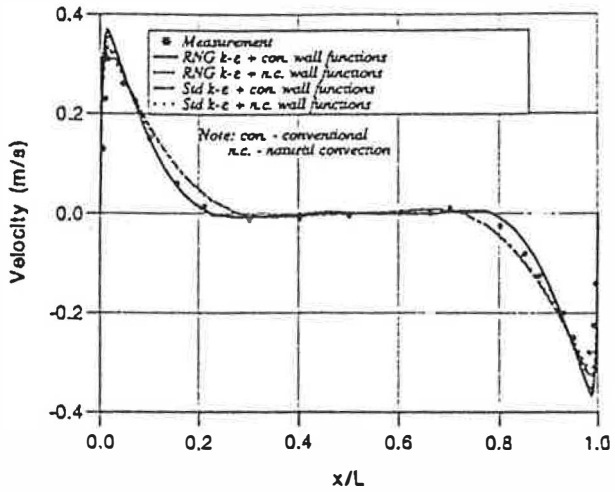

(*a*)

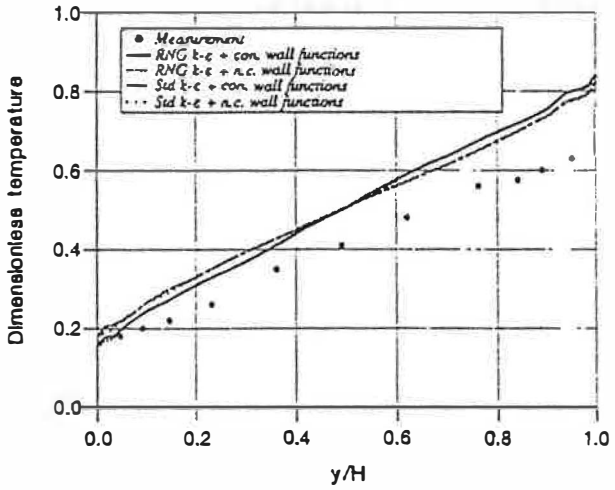

(*b*)

Figure 6. Predicted (*a*) velocity at midheight and (*b*) core temperature in the 5:1 cavity.

tions by the standard k-ϵ model. However, similar to the flow in the narrow cavity, the predicted maximum velocities using the RNG k-ϵ model are higher than those using the standard k-ϵ model.

The predicted core temperature for the cavity is compared with the measurement in Figure 6*b*. The lower measured temperature shown in the figure may be attributed to the imperfect insulation during the experiment. The vertical gradient of the temperature profiles predicted by the RNG k-ϵ model is slightly larger than that by the standard k-ϵ model. In terms of wall heat transfer, the estimated Nusselt number at the midheight is 191. This value is obtained using the following

correlation based on the measured data for the heated wall [21]:

$$\mathrm{Nu} = 0.042\mathrm{Ra}_H^{0.385} \qquad \mathrm{Ra}_H > 5.6 \times 10^8 \tag{19}$$

The RNG k-ϵ model (with the conventional wall functions) predicts a corresponding Nu of 221, whereas the standard k-ϵ model gives 230. Although both models overpredict the wall heat transfer, the RNG k-ϵ model performs relatively better than the standard k-ϵ model. The influence of wall functions on the predicted temperature profile and wall heat transfer is negligible. For example, the predicted Nu using the RNG k-ϵ model with the wall functions for natural convection is 219, compared with 221 using the conventional wall functions.

Henkes and Hoogendoorn [22] showed that experimental data for a cavity of such a low aspect ratio (5:1) could be used for validating numerical results in a square cavity at the same Rayleigh number Ra_H. Hence the RNG k-ϵ model can also be applied to prediction of buoyant flow in a square cavity or similar enclosures such as buildings. In such applications, the wall functions for natural convection will perform slightly better than the conventional wall functions for shear flow.

PARAMETRIC ANALYSIS

In this section we analyze the main parameters that result in better predictions of flow in the tall cavities using the RNG k-ϵ model than the standard k-ϵ model. The analysis is performed for the narrow tall cavity at $\mathrm{Ra}_L = 0.86 \times 10^6$ using the RNG k-ϵ model with the conventional wall functions. Table 2 presents a summary of the predicted results.

Table 2. Effect of variable turbulence parameters in the RNG k-ϵ model on the results at midheight of narrow cavity ($\mathrm{Ra}_L = 0.86 \times 10^6$)

Parameter	V_{min}, m/s	V_{max}, m/s	Nu_c	Nu_h	T_1, °C
Measurement	−0.135	0.139	6.24	5.91	21.7
Original RNG k-ϵ	−0.135	0.136	6.99	6.83	21.7
$R = 0$	−0.166	0.168	6.23	6.11	21.4
$C_2 = 1.92$	−0.122	0.123	7.40	7.25	21.8
$C_2 = 1.92$ and $R = 0$	−0.137	0.138	6.96	6.81	21.6
$\sigma_k = 1.0$, $\sigma_\epsilon = 1.3$, $\sigma_t = 0.9$	−0.117	0.118	6.92	6.75	21.7
$\sigma_k = 1.0$, $\sigma_\epsilon = 1.3$, $\sigma_t = 0.9$, $R = 0$	−0.146	0.148	6.09	5.97	21.4
$\sigma_k = 1.0$, $\sigma_\epsilon = 1.3$, $\sigma_t = 0.9$, $C_2 = 1.92$	−0.106	0.106	7.35	7.16	21.9
$\sigma_k = 1.0$, $\sigma_\epsilon = 1.3$, $\sigma_t = 0.9$, $C_2 = 1.92$, $R = 0$	−0.119	0.120	6.88	6.71	21.7
$\sigma_k = \sigma_\epsilon = \sigma_t = 0.72$	−0.136	0.137	6.92	6.76	21.7
$\sigma_\epsilon = 1.3$	−0.125	0.126	7.65	7.49	21.7
$\sigma_k = 1.0$	−0.124	0.125	6.97	6.78	21.9
$\sigma_t = 0.9$	−0.139	0.141	6.20	6.08	21.5
$\sigma_k = 1.0$ and $\sigma_\epsilon = 1.3$	−0.112	0.113	7.73	7.54	21.9
$\mu_e = \mu_t$	−0.125	0.126	7.44	7.28	21.8

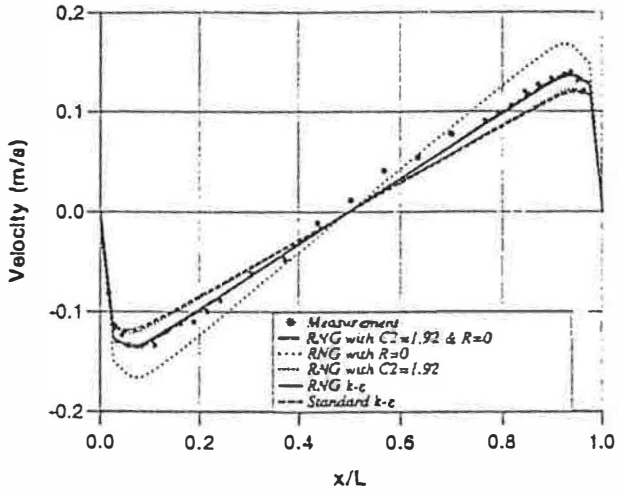

(*a*)

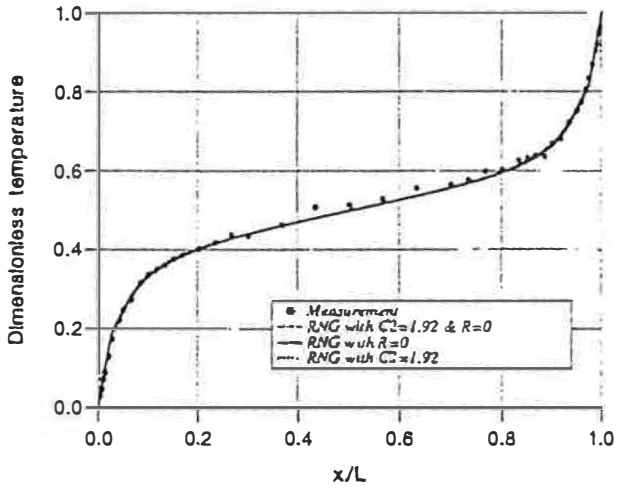

(*b*)

Figure 7. Predicted (*a*) velocity and (*b*) temperature at midheight of the narrow cavity for varying C_2 and R in the RNG k-ϵ model.

First, the turbulence constant C_2 and the rate-of-strain term R in the ϵ equation are varied. Figure 7 shows the predicted velocity and temperature with the variations.

When R is set to zero, the predicted maximum velocity at the midheight is increased considerably, much higher than the measurement. This is the consequence of decreased dissipation and increased turbulent viscosity when R is neglected. Thus the inclusion of the rate-of-strain term decreases the gradient of velocity profile. Yakhot et al. [15] pointed out that the contribution of R in the ϵ

equation was small for weakly strained turbulent flows, and vice versa. Since R has a marked effect on the predicted velocity distribution, it can be postulated that flow near the cavity midheight is strongly strained turbulent.

When the value for C_2 is increased from 1.68 for the RNG k-ϵ model to 1.92, the value for the standard k-ϵ model, the opposite effect on the predicted velocity is produced as compared with setting R to zero. That is, increasing C_2 leads to the reduced maximum velocity and decreased gradient of velocity profile outside the boundary layer. The resulting velocity profile is quite close to the prediction using the standard k-ϵ model.

When R is set to zero and C_2 is taken to be 1.92, the predicted velocity is almost the same as that using the original RNG k-ϵ model, indicating that the effect of varying R offsets that of C_2. Although this combined variation results in the same values of C_2 and R for the standard k-ϵ model, the predicted velocity differs from the prediction using the standard k-ϵ model as seen by comparing relevant curves in Figures 2 and 7. This difference results from different values for turbulent Prandtl numbers σ_k, σ_ϵ, and σ_t in the two turbulence models. In other words, the standard k-ϵ model can produce similar results for the cavity flow to those from the RNG k-ϵ model if the turbulent Prandtl numbers are calculated from Eq. (6).

The difference in the predicted temperature profile for the varying values of R and C_2 is small (Figure 7*b*). Quantitatively, however, the maximum difference in the predicted wall heat transfer is almost 20%, and the difference in the temperature at 0.1 cavity width is about 0.4°C (Table 2). Similar effects of varying σ_k, σ_ϵ, and σ_t on the wall heat transfer and temperature distribution are observed.

Next, the turbulent Prandtl numbers σ_k, σ_ϵ, and σ_t in the RNG k-ϵ model are changed alone or in conjunction with turbulence constants. Figure 8 shows the predicted velocity at the cavity midheight with these variations. When σ_k, σ_ϵ, and

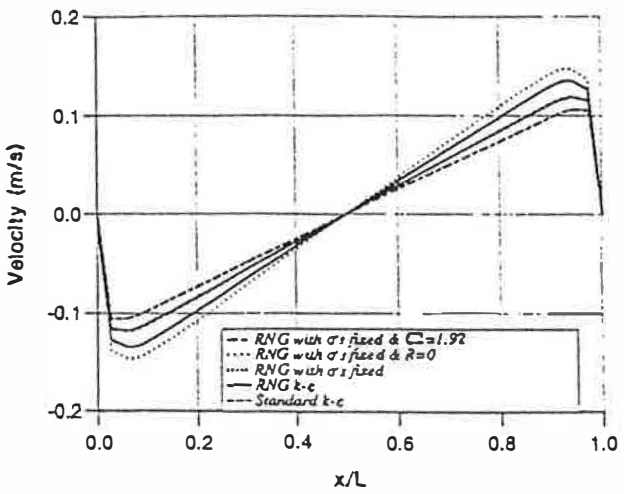

Figure 8. Predicted velocity at cavity midheight with turbulent Prandtl numbers in the RNG k-ϵ model fixed (σ_k = 1.0, σ_ϵ = 1.3, σ_t = 0.9).

σ_t are taken to be the same constants as those for the standard k-ϵ model, the effect on the predicted velocity is similar to the case where the constant C_2 is changed to the value for the standard k-ϵ model. The maximum velocity is slightly lower than the result from the standard k-ϵ model. When this variation is combined with setting R to zero, the predicted velocity profile resembles but the magnitude of velocity is higher than that for the combined change of C_2 and R to values for the standard k-ϵ model. Hence the effect of different values for σ_k, σ_ϵ, and σ_t is larger than that of C_2. When σ_k, σ_ϵ, and σ_t together with C_2 are set to the values for the standard k-ϵ model, the prediction is worsened, with the predicted velocity being the lowest of all the predictions. When all these variations are combined, i.e., σ_k, σ_ϵ, σ_t, R, and C_2 are changed to the values for the standard k-ϵ model, the predicted velocity is almost the same as the prediction using the standard k-ϵ model. This can be seen from Table 2 but is not shown in Figure 8, as the profile would have overlapped the curve for the standard k-ϵ model. The result implies that the effect of C_μ and C_1 for the difference in predictions using the two models is negligible mainly because the difference in C_μ and C_1 between the models is small. This is confirmed by predictions with two values for C_μ and C_1 in the two models, which give little difference between the predicted flow patterns.

When all the turbulent Prandtl numbers are taken to be a constant 0.72 for high-Re flow, the predicted velocity is slightly higher than that using the values given by Eq. (6). The difference between them is, however, insignificant ($\approx$ 1%).

Further predictions show that among these turbulent Prandtl numbers, σ_ϵ affects the predicted velocity at and near the peaks, whereas σ_k and σ_t affect the whole velocity profile (Figure 9). When σ_k is set to 1.0, the predicted velocity profile except for the region near the peaks is very similar to that using the standard k-ϵ model and hence lower than that using the RNG k-ϵ model. Setting σ_t to 0.9 leads to slightly higher velocity than the prediction using the original

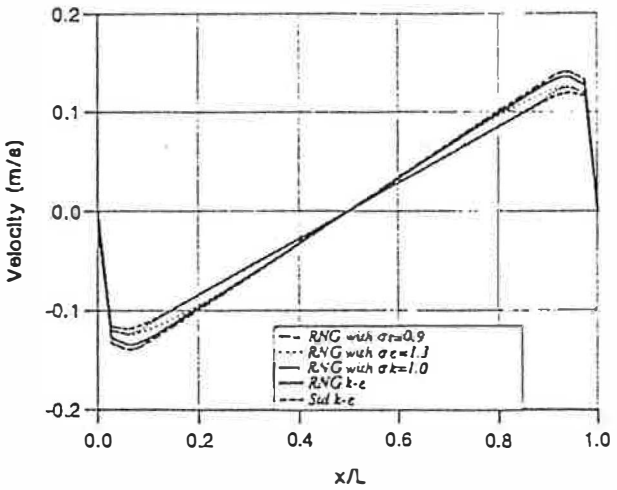

Figure 9. Predicted velocity at cavity midheight for varying turbulent Prandtl numbers in the RNG k-ϵ model.

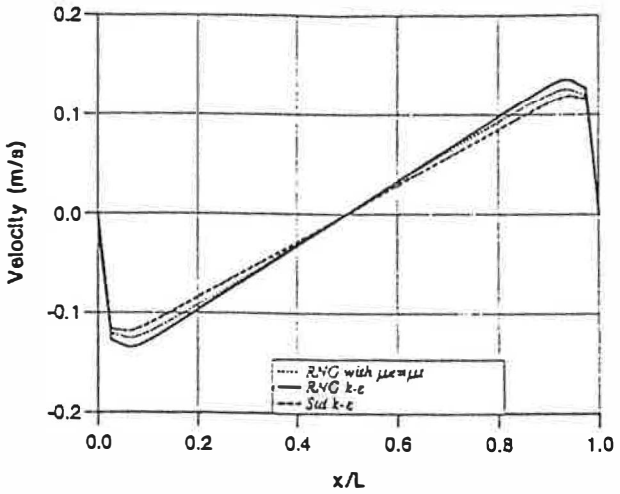

Figure 10. Effect of viscosity on the predicted velocity at cavity midheight.

RNG k-ϵ model. When both σ_ϵ and σ_k are set to the values for the standard k-ϵ model, the velocity at midheight is much underpredicted. Although the difference in σ_k between the two models is smaller than that in σ_ϵ, it has larger influence on overall velocity predictions.

Finally, we investigate the effect of employing the effective or turbulent viscosity for the diffusion term in the k and ϵ equations on the accuracy of prediction. When the effective viscosity is replaced by the turbulent viscosity, which is valid for high-Re flow, the predicted velocity lies between the predictions using the original RNG and standard k-ϵ models (Figure 10). This suggests that there are regions in the cavity where flow is not fully turbulent and that the effective viscosity is more appropriate than turbulent viscosity for the diffusion term in the k and ϵ equations. It also implies the effect of low-Re flow and thus requires the consideration of a low-Re k-ϵ model. However, use of such a model, though without the need of wall functions, does not necessarily improve flow predictions. This is evidenced by the work of Betts and Dafa'Alla [3]. It was shown that none of the available low-Re turbulence models could produce a completely satisfactory result for the same cavity geometry. The most recent work [6] in this area also suggests that low-Re turbulence models still need improving for the accurate prediction of buoyant flows.

The above analysis demonstrates that the principal parameters that result in the improvement of buoyant flow prediction are the coefficients/terms in the ϵ equation, namely, C_2 and R as well as turbulent Prandtl numbers σ_k, σ_ϵ, and σ_t. The expressions for these coefficients form a delicate balance.

CONCLUSIONS

This study shows that for predicting buoyancy-induced turbulent flows the RNG k-ϵ model performs better than the standard k-ϵ model. The improved

13. F. S. Lien and M. A. Leschziner, Assessment of Turbulence-Transport Models Including Nonlinear RNG Eddy-Viscosity Formulation and Second-Moment Closure for Flow over a Backward Facing Step, *Comput. Fluids*, vol. 23, no. 8, pp. 983–1004, 1994.
14. Q. Chen, Comparison of Different k-ϵ Models for Indoor Airflow Computations, *Numer. Heat Transfer, Part B: Fundamentals*, vol. 28, no. 3, pp. 353–369, 1995.
15. V. Yakhot, S. Orszag, S. Thangam, T. B. Gatski, and C. G. Speziale, Development of Turbulence Models for Shear Flows by a Double Expansion Technique, *Phys. Fluids, Part A*, vol. 4, no. 7, pp. 1510–1520, 1992.
16. C. L. V. Jayatillaka, The Influence of Prandtl Number and Surface Roughness on the Resistance of the Laminar Sublayer to Momentum and Heat Transfer, *Progr. Heat Mass Transfer*, vol. 1, pp. 193–329, 1969.
17. S. V. Patankar, *Numerical Heat Transfer and Fluid Flow*, Hemisphere, Washington, DC, 1980.
18. P. G. Huang and M. A. Leschziner, An Introduction and Guide to the Computer Code TEAM, Report TFD/83/9, Department of Mechanical Engineering, UMIST, UK, 1983.
19. P. L. Betts and I. H. Bokhari, Experiments on Turbulent Natural Convection of Air in a Tall Cavity, in *Proc. 5th ERCOFTAC/IAHR Workshop on Refined Flow Modelling, Chatou, Paris*, April 25–26, 1996.
20. P. L. Betts and I. H. Bokhari, New Experiments on Turbulent Natural Convection of Air in a Tall Cavity, in *IMechE Conference Transactions*, C510/091/95, pp. 213–217, 1995.
21. R. Cheesewright, K. J. King, and S. Zia, Experimental Data for the Validation of Computer Codes for the Prediction of Two-Dimensional Buoyant Cavity Flows, *ASME Winter Annual Meeting, Anaheim, California*, HTD-vol. 60, pp. 75–81, 1986.
22. R. A. W. M. Henkes and C. J. Hoogendoorn, Rayleigh-Number, Aspect-Ratio and Prandtl-Number Dependence for Turbulent Natural Convection in Side-Heated Cavities, in *Proc. Eurotherm Seminar 22 on Turbulent Natural Convection in Enclosures*, pp. 257–276, EETI, Paris, 1993.

prediction results mainly from the inclusion of the rate-of-strain term in the ϵ equation. Modifications of the turbulence constants C_2, σ_k, σ_ϵ, and to a lesser extent, σ_t also contribute to the improvement. The RNG k-ϵ model turbulence model is therefore preferable to the standard k-ϵ model for simulating buoyant flows in enclosures. In the simulation the effective viscosity should be used for the diffusion term in the k and ϵ equations.

It is also shown that wall functions derived from data of turbulent natural convection along a vertical plate may not be applicable to the simulation of buoyancy-induced flows in narrow cavities where there could be interference between the boundary layers of opposing walls. When such interference is absent, the wall functions for turbulent natural convection can be used for the simulation of buoyant flows in enclosures. However, application of wall functions for natural convection requires considering the orientation of a wall surface and also direction of heat transfer, and so similar correlations are needed for natural convection along horizontal and inclined wall surfaces.

REFERENCES

1. F. J. K. Ideriah, Prediction of Turbulent Cavity Flow Driven by Buoyancy and Shear, *J. Mech. Eng. Sci.*, vol. 22, no. 6, pp. 287–295, 1980.
2. B. E. Launder and D. B. Spalding, The Numerical Computation of Turbulent Flows, *Comput. Methods Appl. Mech. Eng.*, vol. 3, pp. 269–289, 1974.
3. P. L. Betts and A. A. Dafa'Alla, Turbulent Buoyant Airflow in a Tall Rectangular Cavity, in *ASME Winter Annual Meeting, Anaheim, California*, HTD-vol. 60, 83–91, 1986.
4. N. Z. Ince and B. E. Launder, On the Computation of Buoyancy-Driven Turbulent Flows in Rectangular Enclosures, *Int. J. Heat Fluid Flow*, vol. 10, no. 2, pp. 110–117, 1989.
5. R. A. W. M. Henkes and C. J. Hoogendoorn, Comparison Exercise for Computations of Turbulent Natural Convection in Enclosures, *Numer. Heat Transfer, Part B: Fundamentals*, vol. 28, no. 1, pp. 59–78, 1995.
6. D. Laurence, I. Dauthieu, and S. Richoud, Natural Convection in Tall Cavities, in *Proc. 5th ERCOFTAC/IAHR Workshop on Refined Flow Modelling, Chatou, Paris*, April 25–26, 1996.
7. D. Laurence, Modelling Flows Around Bluff Bodies by Reynolds Averaged Transport Equations, *J. Wind Eng. Ind. Aerodyn.*, vols. 46 and 47, pp. 53–68, 1993.
8. R. A. W. M. Henkes and C. J. Hoogendoorn, Scaling of the Turbulent Natural Convection Flow in a Heated Square Cavity, *J. Heat Transfer*, vol. 116, no. 2, pp. 400–408, 1994.
9. X. Yuan, A. Moser, and P. Suter, Wall Functions for Numerical Simulation of Turbulent Natural Convection Along Vertical Plates, *Int. J. Heat Mass Transfer*, vol. 36, pp. 4477–4485, 1993.
10. R. A. W. M. Henkes and C. J. Hoogendoorn, Numerical Determination of Wall Functions for the Turbulent Natural Convection Boundary Layer, *Int. J. Heat Mass Transfer*, vol. 33, no. 6, pp. 1087–1097, 1990.
11. V. Yakhot and S. Orszag, A Renormalization Group Analysis of Turbulence, *J. Sci. Comput.*, vol. 1, no. 1, pp. 3–51, 1986.
12. Y. Nakamura and A. E. Sakya, Capturing of Transition by the RNG Based Algebraic Turbulence Model, *Comput. Fluids*, vol. 24, no. 8, pp. 909–918, 1995.